Quantitative study of adsorbate-adsorbate interactions of hydrogen on the Si(100) surface

Zonghai Hu, Albert Biedermann,* Ernst Knoesel,† and Tony F. Heinz
Departments of Physics and Electrical Engineering, Columbia University, New York, New York 10027, USA
(Received 17 October 2002; published 20 October 2003)

The equilibrium spatial distribution of hydrogen atoms adsorbed on the clean Si(100)-2×1 surface under ultrahigh vacuum conditions has been investigated by means of scanning tunneling microscopy (STM). Singly occupied dimers, doubly occupied dimers, and clusters of adjacent doubly occupied dimers along a dimer row are observed. Through the evaluation of large-area STM images, a quantitative assessment of the prevalence of the different adsorbate configurations has been obtained for a range of hydrogen coverages from 0.03 to 0.59 monolayers. At moderate coverages, most of the hydrogen adatoms are found in doubly occupied dimers, while a relatively small number are present as singly occupied dimers or as part of clusters of doubly occupied dimers. The interaction between doubly occupied dimers was examined by determining the experimental size distribution of clusters and the spatial correlation function for the doubly occupied dimers. A nearest-neighbor interaction model is compared with experiment within analytic approximations and through full Monte Carlo simulations. The model is found to agree well with the experimental results. An effective pairing energy of $\varepsilon = 0.31 \pm 0.04$ eV and an effective clustering energy of $\omega = 0.04 \pm 0.01$ eV are inferred. These results are independent of any hypothesis concerning the adsorption/desorption pathways, but have implication for possible pathways and their kinetics.

DOI: 10.1103/PhysRevB.68.155418 PACS number(s): 68.35.Md, 68.37.Ef, 82.20.Wt, 82.40.Ck

I. INTRODUCTION

The system of H/Si(100)-2×1 has been the subject of considerable attention over the past years because of its technological relevance and its inherent scientific interest as model for chemisorption on a covalently bonded surface. With respect to the former, it may be noted that the interaction of hydrogen with silicon surfaces is significant in the growth of silicon films by chemical vapor deposition. Indeed, in certain regimes hydrogen desorption is the rate-limiting step for the growth of epitaxial silicon films.[1] In addition, the role of hydrogen in passivation of silicon surfaces imports additional importance to this system.[2]

From the perspective of fundamental surface science, H/Si(100) is attractive because of the simplicity of the clean H/Si(100)-2×1 surface and of adsorbed species. In particular, at low adsorbate coverages, hydrogen is present in a monohydride phase and binds through an interaction with a dangling bond of the reconstructed surface, without any dramatic change in the underlying Si surface structure. This basic outline of the features of the system is well understood. Despite this apparent simplicity, the system still presents many intriguing features. Particularly noteworthy are the characteristics of adsorption and desorption of molecular hydrogen on this surface. The dissociative adsorption process exhibits a dramatic enhancement in efficiency with increasing surface temperature, an effect that has come to be known as phonon-assisted sticking.[3,4] Thermal desorption of hydrogen also exhibits unexpected features. Particularly striking is the strong departure from the expected second-order kinetics observed for the recombinative desorption process.[5–7]

Fundamental to consideration of these phenomena and of obvious intrinsic interest is the question of the equilibrium structure of the adsorbate-covered surface. For fractional adsorbate coverage, the hydrogen atoms are not arranged randomly among the available dangling-bond sites. They are found rather to exhibit a strong propensity to occupy a pair of dangling bonds on a single dimer. The driving force for this pairing effect lies in the π bond formed between the two Si atoms of a clean dimer.[8,9] This π bond is disrupted when one H atom is adsorbed on the dimer. Thus two H atoms on distinct dimers prefer to occupy a single dimer, which permits the system to recover the energy of one of the two disrupted π bonds. This effect leads to an effective H-H pairing energy ε, which is defined as the energy required to unpair the two hydrogen atoms on a single dimer, that is, to change one doubly occupied dimer and an empty dimer into two singly occupied dimers. Direct evidence for H pairing was found in an early study by scanning tunneling microscopy (STM).[10] The unusual kinetics for the recombinative desorption of adsorbed H atoms was also taken to suggest the importance of hydrogen pairing on dimers. Contrary to what would normally be expected for the production of hydrogen molecules from the recombinative desorption of pairs of adsorbed hydrogen atoms, researchers found that the desorption rate for a significant range of hydrogen coverage followed approximately first-order kinetics.[5–7] A natural explanation for this behavior was found in a ''prepairing'' mechanism.[7] In this scheme, desorption occurs only from the hydrogen atoms of doubly occupied dimers. Thus if the adsorbed hydrogen atoms are strongly paired on the surface under equilibrium conditions, first-order kinetics may be expected for the desorption process. From analysis of temperature-programmed desorption measurements within this picture, a pairing energy of about 0.3 eV was obtained by D'Evelyn and co-workers.[11] In first principle calculations, results of comparable magnitude of 0.08,[12] 0.22,[13] and 0.25 eV (Ref. 14) were obtained. Isothermal desorption measurements by Höfer *et al.*[6] revealed a departure from first-order desorption kinetics at hydrogen coverages below 0.1 monolayer. These results were interpreted in terms of the entropy-driven unpairing of doubly occupied dimers. The kinetics at

high and low coverages could then be fit using a lattice-gas model with a pairing energy of 0.25 eV.

An effective attractive interaction between adjacent doubly occupied dimers has also been considered. Such an interaction would arise from an interdimer π bond, the existence of which was suggested by early experimental[15–17] and theoretical[18–20] investigations showing dispersion of the surface valence band along the direction of the dimer rows. In analogy to the intradimer π bond discussed above, we would then expect that adjacent doubly occupied dimers would be more energetically favorable than two separated doubly occupied dimers, since in the former case, the number of disrupted interdimer bonds would be 3, while in the latter case it would be 4. The effective clustering energy, denoted by ω, is defined as the energy required to separate two adjacent doubly occupied dimers, that is, to transform two adjacent doubly occupied dimers into separated doubly occupied dimers. The early STM investigations of Boland[10] exhibited evidence for such an interaction between doubly occupied dimers: A clustering phenomenon was observed in which there was a propensity for doubly occupied dimers to group together in one-dimensional chains along the dimer row direction.

This clustering interaction was integrated into more refined intradimer desorption models.[21,22] Yang and D'Evelyn performed Monte Carlo simulations[21] that included both pairing and clustering interactions. By comparing the cluster-size distribution from simulations with the distribution extracted from an STM image obtained by Boland,[10] they obtained an estimate of the pairing energy ε of $\sim$0.2 eV and of the clustering energy ω of $\sim$0.15 eV. Flowers *et al.*[22] performed thermal desorption spectroscopy experiments and similar Monte Carlo simulations. They inferred pairing and clustering energies both of $\sim$0.14 eV. But the discussion about these quantities remains open since the abovementioned Monte Carlo simulations failed quantitatively to reproduce the cluster-size distribution in the STM image obtained by Boland.[10] The values obtained in first-principle calculations for the clustering energy span a large range from 0.06,[23] 0.08,[24] to 0.3 eV.[25] More importantly, recent evidence of the interdimer pathway[26–29] brought clustering into the focus of the discussion of the desorption kinetics. A recent model explains the near-first-order kinetics on the basis of two interdimer desorption/adsorption pathways.[23,29] The clustering effect is relevant if these interdimer pathways are important.

The interaction energies for pairing and clustering are clearly important for the understanding of the surface electronic structure and the hydrogen desorption/adsorption processes. Hence there is a need for accurate information on these interactions, data that are obtained by experimental methods that make no assumption on the pathways for hydrogen desorption/adsorption processes. It is the task of the present work to apply STM to provide direct and detailed information on the equilibrium configurations of hydrogen adatoms on the Si(100)-2×1 over a wide range of adatom coverages. These results permit us to examine the degree of pairing and clustering. The clustering phenomenon is characterized by measuring the fraction of doubly occupied dimers that are adjacent to another doubly occupied dimer. In addition, a more detailed description of the clustering effect is obtained from the experimental data by a determination of the cluster-size distribution and the experimental correlation function. The measurements, which reveal a strong propensity for hydrogen pairing and a weak, but observable, clustering effect, are compared with the prediction of a nearest-neighbor interaction model. We find that this simple model can reproduce all of the experimental observations. While information on the average number of pairing and clustering interactions can be obtained from an analytic solution of the statistical mechanics problem, information about the cluster-size distribution must be extracted from the model by means of a Monte Carlo simulation. We further present a discussion of the spatial correlation function for doubly occupied dimers, an analytic solution of which is possible in the limit of strong pairing interactions (no singly occupied dimers). Good agreement between experiment and theory is also obtained for the spatial correlation function. From these analyses, we infer a value for the effective pairing energy of $\varepsilon = 0.31 \pm 0.04$ eV and an effective clustering energy of $\omega = 0.04 \pm 0.01$ eV. We compare these results with earlier studies and discuss the expected consequences on the hydrogen desorption kinetics.

II. EXPERIMENTAL PROCEDURE

The experiments were carried out in an ultrahigh vacuum (UHV) chamber at a base pressure below 1.0×10^{-10} Torr. Since the principal species in the residual gas was molecular hydrogen, sample purity could be maintained at a very high level for several hours. The chamber was equipped with capabilities for Auger electron spectroscopy (AES), quadrupole mass spectrometry (QMS), and temperature programmed desorption (TPD). A commercial UHV STM was used to take the images. The silicon samples ($12\times2\times0.25$ mm^3) were cut to the desired (100) orientation with an accuracy of $\pm0.25°$. To check for the possible influence of doping, we performed measurements on both *n*- and *p*-type samples using a phosphorous-doped sample with a resistivity of 3 Ω cm and a boron-doped sample with a resistivity of 10 Ω cm. We found out that these two types of samples led to indistinguishable experimental results in the studies reported below. Sample heating was provided by directly passing a current through the sample. The relation between the sample temperature and the heating current was established in advance by using a thermocouple attached to the back of the sample. The estimated error in our temperature calibration for annealing was ±20 K.

Careful preparation of the silicon samples was critical for this study since some of the possible defects are very difficult to distinguish from certain configuration of adsorbed hydrogen atoms. We found that the following procedure produced the highest quality Si(100) surfaces. After initial cleaning by washing with methanol (99.9% purity), the sample was introduced into the UHV chamber. The sample was then heated to a temperature of 1350 K. This heating cycle not only led to the sublimation of the oxide layer, but also caused desorption of surface carbon atoms, an otherwise

problematic contaminant. To obtain highly ordered surfaces, we found that it was crucial to cool the sample slowly. Typically, the sample was brought back to room temperature at a rate of 0.8 K/s. From direct STM analysis, we determined that this procedure for sample preparation produced surfaces with a total density of impurities and structural defects (such as missing dimers, Si islands, and steps) below 0.5%.

Hydrogen was adsorbed on the surfaces by dosing with atomic hydrogen formed from dissociation of H_2 by a hot tungsten filament. We prepared surfaces with a range of different hydrogen coverages from 0.03 monolayers (ML) to 0.59 ML, where 1 ML corresponds to the surface density of Si atoms. After hydrogen adsorption, the surface was carefully annealed to allow the hydrogen-covered surface to reach its equilibrium state. STM images were then obtained after the sample had been brought back to room temperature. Tunneling currents of roughly 0.5 nA and sample bias voltages around -2 V were chosen to record the STM images. Under these scanning conditions, no STM-induced changes of the adsorbate configuration were observed.

An important question for our sample preparation technique is whether surfaces were truly in their equilibrium state, with the different hydrogen configurations corresponding to their fully equilibrated thermal distribution. To address this issue, we prepared samples following different annealing protocols and compared the resulting surface configurations of the adsorbed hydrogen atoms. In these studies, we varied the annealing temperature between 400 and 700 K, with a range of annealing times of 10–6000 s. By comparing the STM images, we concluded that annealing at 570 K was sufficient for the hydrogen ''pair'' configuration to reach equilibrium, but not for full equilibration of ''cluster'' configurations. At increased annealing temperatures in the range of 650 K (just below the onset of hydrogen desorption), we found that evidence for full equilibration: Clustering of hydrogen dimers was clearly present, but its prevalence did not grow with increased annealing times as high as 5000 s. This result is compatible with previous experimental data on hydrogen diffusion on the Si(100) surface.[30,31] According to these investigations, at reasonable surface coverages of hydrogen, pairs of hydrogen atoms will meet other pairs and form clusters at a temperature of 650 K for annealing times of 2000 s. To ensure that full equilibration was achieved, we employed annealing times of roughly 1 h.

A further issue relating to the annealing process concerns the effective surface temperature of the adsorbate configuration observed in the STM measurements. Let us assume, as argued above, that a surface temperature of 650 K permits us to obtain full equilibrium. We would then observe the adsorbate-site distribution corresponding to this temperature in our room-temperature STM measurements only for rapid quenching of the surface. In fact, our cooling rate for the sample was approximately 2 K/s. Thus, some reequilibration at a lower surface temperature may be expected. Given the diffusion rate relevant for cluster formation, we expect this effect to be very slight for the concentration of this species. Indeed, the average hopping times of paired hydrogen atoms is estimated to be less than one hop before the temperature cools to the point where the surface hydrogen is clearly frozen.[30,31] For the more facile motion of hydrogen atoms to form and break doubly occupied dimers, changes in the surface configuration during cooling are of greater relevance. The lowest estimate of the effective surface temperature for this degree of freedom would be 570 K, corresponding to freezing temperature for *all* adsorbate motion.[30,31] Using the measured hopping rates,[30,31] we estimate an effective surface temperature for hydrogen atom pairing of 600 K, approximately 10% below our surface annealing temperature.

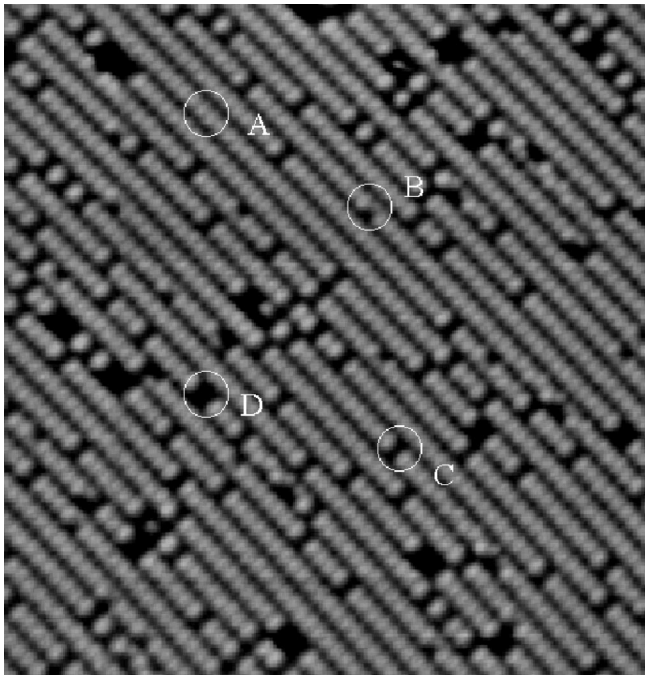

FIG. 1. A representative filled-state STM image of the annealed Si(100) surface with hydrogen adsorbed at a coverage of $\theta = 0.13$ ML. This 20 nm$\times$20 nm image was taken at a sample bias of -2.0 V and a tunneling current of 0.5 nA. The circled regions indicate different configurations of the adsorbed hydrogen sites. A corresponds to an unoccupied dimer, B contains a singly occupied dimer, C a doubly occupied dimer, and D a (size-2) cluster of two adjacent doubly occupied dimers.

III. EXPERIMENTAL RESULTS

A. STM images

Figure 1 shows a filled-state STM image of a Si(100) surface with adsorbed hydrogen atoms at a coverage of 0.13 ML. The brighter features correspond to dangling bonds of unoccupied silicon atoms. Sites with adsorbed hydrogen atoms appear as dark features because of the reduced tunneling current from the Si-H bond state compared to that from the dangling-bond state. Unoccupied dimers, singly occupied dimers, doubly occupied dimers, and clusters of doubly occupied dimers are all clearly resolved in this image. In our experiments, we prepared Si(100) surfaces at a variety of hydrogen coverages θ. At each chosen coverage many large-scale images similar to Fig. 1 were obtained.

As mentioned above, the propensity of adsorbed hydrogen atoms to form doubly occupied dimers and for these doubly

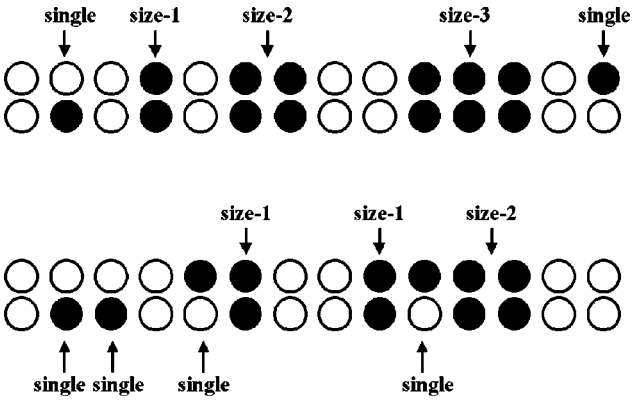

FIG. 2. A schematic diagram illustrating different hydrogen configurations in two representative dimer rows of a Si(100) surface. There are in total $n=28$ dimers, $n_1=6$ singly occupied dimers, and $n_2=10$ doubly occupied dimers. Among doubly occupied dimers, there are $n_2^{(1)}=3$ of "size 1," $n_2^{(2)}=2$ of "size 2," and $n_2^{(3)}=1$ of "size 3."

occupied dimers to cluster along the direction of the dimer rows has been previously reported. The quantification and analysis of this effect is the subject of the present paper. We did, however, also search for correlations between the positions of adsorbed hydrogen atoms in neighboring dimer rows of the Si(100)surface. We did not find any indication of significant interactions across dimer rows. Consequently, our analysis and discussion concerns only behavior observed along a single row of Si dimers.

B. Nomenclature for image analysis

In order to characterize the adsorbate/adsorbate interactions quantitatively, we introduce some appropriate variables to summarize the configuration of adatoms along a row of Si dimers. Let us consider a region of the Si(100) surface consisting of a total of n Si dimer sites (or $2n$ surface Si atoms). We then denote by n_1 the number of dimers occupied by a single H adatom and by n_2 the number of doubly occupied dimers. Among the doubly occupied dimers, we describe those that are not adjacent to another doubly occupied dimer as being a cluster of size 1. If exactly two doubly occupied dimers are adjacent to one another, this configuration comprises a cluster of size 2, and so on. Correspondingly, we denote the number of clusters of size i within the designated area of the surface as $n_2^{(i)}$, where $i=1,2,3\ldots$. Some of the possible adsorbate configurations within a dimer row are indicated schematically in Fig. 2. The total number of doubly occupied dimers is given simply as a sum over clusters of each size i:

$$n_2=\sum_i i\times n_2^{(i)}. \tag{1}$$

Another useful quantity is the number, which we denote as n_{22}, of clustering "bonds" present between adjacent doubly occupied dimer sites. In terms of the number $n_2^{(i)}$ of clusters of each size i, it can be expressed as

$$n_{22}=\sum_i (i-1)\times n_2^{(i)}, \tag{2}$$

From these numbers observed for different surface configurations, we then express the prevalence of the various H-atom configurations in normalized units of coverage. The coverage of hydrogen atoms corresponding to singly occupied and doubly occupied dimers can be described as $\theta_1=n_1/(2\times n)$ and $\theta_2=n_2/n$, respectively, with a total hydrogen adatom coverage of $\theta=\theta_1+\theta_2$. The partial coverage of doubly occupied dimers in clusters of size i is then $\theta_2^{(i)}=i\times n_2^{(i)}/n$. We also define the fraction of doubly occupied dimers residing in clusters of size i as $f_2^{(i)}=\theta_2^{(i)}/\theta_2$. For our later analysis, we introduce the coverage of clustering "bonds" as $\theta_{22}=n_{22}/n$.

C. Counting results for size distributions

Experimental values for the prevalence of the different configurations of the adsorbed hydrogen described above were determined by direct analysis of the STM images. We recorded, for each hydrogen coverage θ, a sufficient data set to permit analysis of $n\sim 3\times 10^4$ sites. This procedure ensured good statistical accuracy for the quantities of interest by direct counting. The principal source of uncertainty in the experiment actually arose from the presence of surface defects and impurities. Despite considerable effort to obtain very high quality surfaces, defects need to be considered, particularly in the regime of low adsorbate coverage. Defects that could be differentiated from possible configurations of adsorbed H could be neglected. Some of the defects and impurities, however, could not be distinguished from singly or doubly occupied dimers. The corresponding coverages, which could be determined by examining the surface prior to hydrogen dosing, were found to be less than 0.2 and 0.3 %, respectively. The resulting error in our counting of the cluster-size distribution $n_2^{(i)}$ was found small compared statistical uncertainties and was neglected. With respect to the number of singly occupied dimers n_1 however, the experimental data were corrected by subtraction of the estimated 0.2% contribution from the presence of defects and impurities.

The results from analysis of the STM images are shown in Fig. 3 for a range of hydrogen coverage θ from 0.03 to 0.59 ML. In this figure, we indicate for each total hydrogen coverage θ, the coverage θ_1 of hydrogen in singly occupied dimers. The corresponding coverage of doubly occupied dimers is $\theta_2=\theta-\theta_1$. The partial coverages of H in clusters of different sizes $\theta_2^{(i)}$ is plotted as the fraction $f_2^{(i)}=\theta_2^{(i)}/\theta_2$ of hydrogen in cluster size $i=1,2,3,4,5,6+$. The data for clusters of length 6 and greater have been grouped together $(i=6+)$, since adequate statistical accuracy could not generally be obtained for clusters of size $i>6$. The solid lines in Fig. 3 are the results of the Monte Carlo simulation described in Sec. IV D below.

An alternative presentation of some of the data in Fig. 3 is given in Fig. 4. Figure 4(a) plots the coverage θ_2 of doubly occupied dimers as a function of the total hydrogen coverage θ. Figure. 4(c) plots the corresponding result for the coverage θ_1 of hydrogen atoms in singly occupied dimers. Figure

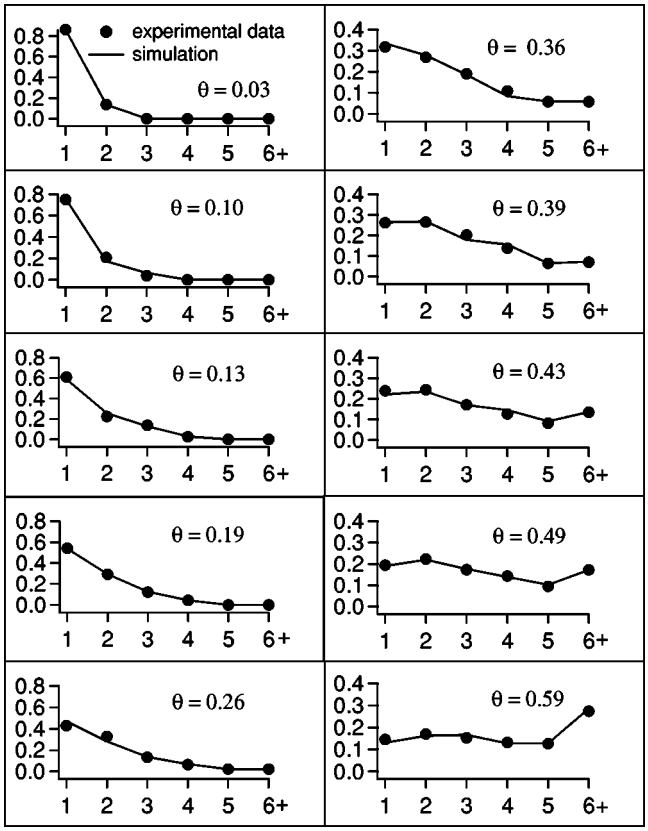

FIG. 3. Summary of data for the cluster-size distribution for a range of different coverages θ (in ML) of adsorbed hydrogen. For each value of θ, the dots represent the experimental value for the fraction $f_2^{(i)}$ of paired hydrogen atoms in clusters of size $i=1,2,3,4,5,6+$, where $6+$ includes all clusters of size 6 or greater. The statistical errors (not shown) are smaller than the size of the data points. The corresponding values for the coverage of hydrogen in singly occupied dimers is $\theta_1=0.005$ ML for $\theta=0.03$ ML, $\theta_1=0.011$ ML for $\theta=0.10$ ML, $\theta_1=0.014-0.016$ ML for higher values of θ [see Fig. 4(c)]. The solid lines are predictions of the quasi-one-dimensional nearest-neighbor interaction model discussed in the text. The model is evaluated by a Monte Carlo simulation (Sec. IV D) with a fixed choice of $\varepsilon/kT=6.1$ and $\omega/kT=0.8$ for all coverage θ.

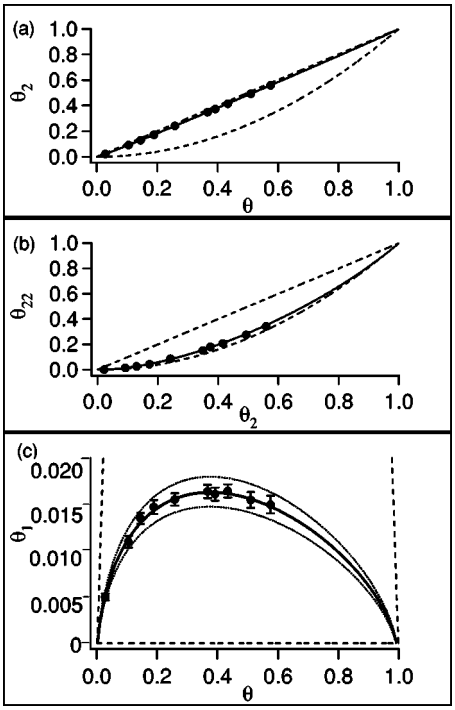

FIG. 4. Comparison of experimental data for the coverage of hydrogen pairing and clustering "bonds" (points with error bars from counting statistics) with calculated results (lines). (a) The coverage of doubly occupied dimers θ_2 vs the total hydrogen coverage θ. The upper and lower dotted curves correspond, respectively, to complete pairing and no pairing interaction. The solid curve gives the predictions of the statistical model with parameters $\varepsilon/kT=6.1$ and $\omega/kT=0.8$. (b) The coverage of clustering "bonds" between adjacent doubly occupied dimers θ_{22} vs the coverage of doubly occupied dimers θ_2. The upper and lower dotted curves correspond, respectively, to complete clustering and no clustering interaction. The solid curve gives the predictions of the statistical model with $\varepsilon/kT=6.1$ and $\omega/kT=0.8$. (c) Coverage of singly occupied dimers $\theta_1=\theta-\theta_2$ vs total H coverage θ. The dashed lines correspond to infinite interaction (horizontal line) and no interaction (nearly vertical lines). The thick solid curve displays the predictions of the statistical model with $\varepsilon/kT=6.1$ and $\omega/kT=0.8$. The other two curves correspond to ε/kT varied by ± 0.6.

4(b) shows the experimentally determined coverage of cluster "bonds" $\theta_{22}=n_{22}/n$. This quantity provides, as discussed below, a convenient measure of the effective interaction between adjacent doubly occupied dimers.

D. Correlation function for doubly-occupied dimers

One approach to investigate the interaction between doubly occupied dimers is the characterization of the distribution of cluster sizes, as just presented. An alternative scheme of data analysis involves the determination of the spatial correlation function. As discussed below in Sec. IV C 2, this approach permits comparison with an analytic solution of a statistical mechanical treatment of nearest-neighbor adsorbate-adsorbate interactions for the doubly occupied dimers. The spatial correlation function for the doubly occupied dimers along a dimer row is found from the experimental data in the following fashion. For each doubly occupied dimer, we write down the site occupancy $P(j)$ of dimers removed by a displacement of j dimer units along the dimer row, where $P(j)=1$ for a doubly occupied dimer at displacement j and $P(j)=0$ otherwise. The spatial correlation function $p(j)$ is then given as $p(j)=\langle P(j)\rangle$, where the ensemble average is computed using all available doubly occupied dimers in the experimental STM images. We neglected sites located near the edge of the recorded STM image, as well as those near steps and other identifiable defects. Since the behavior is symmetric for displacements in either direction along a dimer row, we folded together displacements j of negative and positive sign. Figure 5 shows experimental results for the spatial correlation function measured at two different adsorbed H coverages of $\theta=0.13$ and 0.26 ML. Note that for the purpose of this analysis, we have treated sites that contain a singly occupied dimer as being unoccupied. In fact,

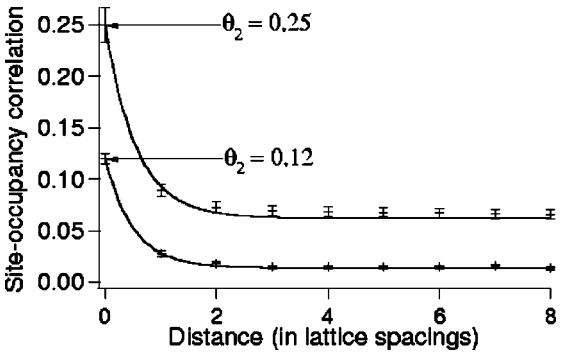

FIG. 5. Experimental data of correlation function of doubly occupied dimers. The horizontal is distance in units of the lattice constant along the dimer row. The solid curves are the best fits to the one-dimensional Ising model (described in Sec. IV C 2) with the value of $\omega/kT=1.0$ for the clustering energy at coverage of $\theta=0.13$ ML and $\omega/kT=0.9$ at coverage of $\theta=0.26$ ML. The error bars are based on counting statistics.

there is a small fraction of unpaired H adatoms. The corresponding values for $\theta_2=\theta-\theta_1$ are 0.12 and 0.25 ML for the conditions of the two measurements.

IV. ANALYSIS

In this section, we first present, in part A, a qualitative discussion of the experimental data and a comparison with simple limiting behavior for weak and strong adsorbate-adsorbate interactions. We then discuss, in part B, a simple quasi-one-dimensional model for the interaction of adsorbed hydrogen atoms that has been previously introduced in the literature. Within this model, we can compare with experiment the predictions for hydrogen coverages θ_1 and θ_2 in singly and doubly occupied dimers and for the coverage θ_{22} of the clustering bonds between doubly occupied dimers. Good agreement for these data with fixed values for the pairing and clustering energies is found over the observed range of total hydrogen coverage θ. A further comparison with an analytic result is possible if we consider only the nearest-neighbor interaction of the doubly occupied dimers. As we also discuss in part C, an expression for the spatial correlation function of the doubly occupied dimers is available and is found to provide quite satisfactory agreement with the correlation functions determined experimentally. The most complete set of experimental data is that of the cluster-size distribution measured for various values of the hydrogen coverage θ. To reproduce these results, we present in part D a full Monte Carlo simulation of the quasi-one-dimensional model and extract thereby values for the two relevant interaction energies.

A. Qualitative observations

The general character of the effective H adsorbate-adsorbate interactions on the Si(100) surface can be understood by reference to the results shown in Fig. 4. With respect to the effective pairing interaction between two hydrogen atoms on a single dimer, it is instructive to examine Fig. 4(a). For complete pairing, we would obtain $\theta_2=\theta$, all hydrogen being found in doubly occupied dimers. On the other hand, with no adsorbate-adsorbate interaction whatsoever, there will only be a statistical chance of finding two hydrogen atoms on the same dimer, i.e., $\theta_2=\theta^2$. Inspection of Fig. 4(a) reveals that the data lie relatively close to the complete pairing limit of $\theta_2=\theta$. There is, however, a clear departure from this extreme limit for which the coverage of singly occupied dimers θ_1 approaches zero. The existence of incomplete pairing is highlighted in Fig. 4(c), which displays θ_1, or the coverage of *unpaired* hydrogen, as a function of θ. From these consideration one may immediately conclude that the effective pairing interaction is significant compared to the thermal energy scale (at the annealing temperature), but is not overwhelmingly larger.

The situation for the effective interaction between doubly occupied dimers is reflected in Fig. 4(b). If we assume for simplicity that essentially all of the hydrogen is found in doubly occupied dimers, then the coverage of dimer bonds, θ_{22}, would scale as $\theta_{22}=\theta_2$ for complete clustering and as $\theta_{22}=\theta_2^2$ for a negligible interaction between the doubly occupied dimers. In this case, the data actually lie quite close to the non-interacting limit of $\theta_{22}=\theta_2^2$. This suggests that the interaction energy is not large compared to the thermal energy. That there is a finite (attractive) interaction, however, is apparent from the fact that the experimental values for θ_{22} fall consistently above the noninteracting limit of $\theta_{22}=\theta_2^2$.

B. A quasi-one-dimensional model of adsorbate-adsorbate interactions

In order to analyze the data in a more quantitative fashion, we clearly need to introduce a definite model of the effective interactions between the adsorbed hydrogen atoms. We make use of the simplest model that is capable of explaining the observed pairing of hydrogen atoms on a single dimer and the (modest) propensity of doubly occupied dimers to form clusters along a dimer row. This model, previously presented in this context by D'Evelyn *et al.*[21] and Flowers *et al.*,[22] is quasi-one-dimensional in character and describes the behavior along one row of Si dimers. As mentioned above, no experimental evidence of significant interactions between the dimer rows was found.

In the model we include an effective pairing energy ε and an effective clustering energy ω. These quantities are defined in the following fashion. As mentioned in the Introduction, the pairing energy ε is the energy required to transform two hydrogen atoms on an isolated doubly occupied dimer into two separated hydrogen atoms on different dimers. We further assume that this energy is identical for separating the hydrogen atoms by one dimer or more, i.e., that it is a nearest-neighbor interaction. The clustering energy ω is the analogous quantity for transforming an isolated pair of adjacent doubly occupied dimers into separated doubly occupied dimers. This interaction is also assumed to be significant only for nearest neighbors and is treated as strictly additive. Thus, a cluster of size 3 will have an interaction energy of -2ω relative to hydrogen atoms on separated doubly occu-

pied dimers. Within this model, we see that the overall interaction energy of a given adsorbate configuration per surface atom can then be given by

$$E = \theta_1 \varepsilon/2 + (\theta - \theta_{22})\omega/2. \quad (3)$$

Here the zero of energy corresponds to a configuration where all of the hydrogen atoms are in adjacent doubly occupied dimers, the lowest available energy configuration.

For simplicity, the interaction between a doubly occupied dimmer and an adjacent singly occupied dimer is neglected within the model, as is the interaction between adjacent singly occupied dimers. The validity of this assumption is hard to gauge and, in the simplest analysis, depends on what factors dominate the interaction between adjacent dimers. In one picture, the interaction might be interpreted as related to the electronic interaction between possible π-bonded dimers, as discussed above. In this case, one would actually lose most of the favorable interaction whenever either dimer is at least partially occupied by hydrogen. Within the model, this would correspond to treating the interaction between any pair of partially or fully occupied dimers as equivalently attractive. On the other hand, one might attribute the effective interaction to strain effects associated with modification of the dimer width by hydrogen adsorption. Depending on the assumptions, this would lead to differing conclusions about effective interactions between fully and partially occupied dimers. In the work of Zimmermann and Pan,[23] different effective interaction strengths are estimated from *ab initio* calculations for all possible configurations of adjacent dimers. The effective interaction energy between two singly occupied dimers is found to be small, while the effective interaction energy between singly and doubly occupied dimers is found to be half of that of a pair of doubly occupied dimers. For the purposes of our current study, there would appear to be relatively little difference between the consequences of such possible variants of the model, since typically relatively few of the adsorbate-adsorbate interactions involve singly occupied dimers. Possible corrections would be expected to be most pronounced in examining clustering effects in the low-coverage regime, which is quite challenging experimentally. Further investigation of these points from the perspective of modeling would, however, be very valuable and a useful subject for future study.

In the following, we apply the nearest-neighbor interaction model to analyze the site occupancy of the H/Si(100) surface. In doing so, we treat the problem as a quasi-one-dimensional lattice gas and neglect any internal degrees of freedom of the system. As indicated in the analysis of Flowers *et al.*,[22] the statistical mechanical analysis would then include additional terms related to the full partition function of the system. The most apparent omission concerns the vibrational degrees of freedom of the adsorbed hydrogen atoms in the different configurations. This factor could, to an extent, be addressed through the use of the known frequencies of the different vibrational modes of the adsorbed hydrogen atoms.[32,33] While distinct frequencies are expected for distinct adsorbate configurations, the differences are not expected to be overwhelmingly large, as indicated, for example, by the influence of adsorbed oxygen on hydrogen vibrational frequencies.[33–35] Further, for the relevant range of temperatures (up to the annealing temperature), relatively weak excitation of hydrogen vibrational modes is expected. What is less easy to quantify would be the influence of the configuration of adsorbed hydrogen on the vibrational modes of the Si atoms in the dimer. In this case, the vibrational modes would be thermally excited and some shift in frequency would be anticipated in view of the changes in the structure of the dimers induced by H adatom adsorption. This effect is neglected in our analysis.

C. Quantitative treatment with analytical methods

1. Coverage of pairing and clustering "bonds"

Within the model introduced above, the surface properties are determined by the two effective interactions energies, ε for pairing and ω for clustering, for any specified total hydrogen coverage θ and surface temperature T. As discussed in Ref. 21,22, one may obtain from statistical mechanics analytic expressions defining the coverage of pairing bonds θ_2 and of cluster bonds θ_{22}. These coverages are defined implicitly by the following two relations:

$$e^{-(\varepsilon+\omega)/kT} = \frac{(\theta - \theta_1)\theta_1^2(1 - 2\theta + 2\theta_1 + \theta_{22})}{\theta_{22}(1 - \theta + \theta_1)^2(1 - \theta - \theta_1)}, \quad (4)$$

$$e^{-\omega/kT} = \frac{(\theta - \theta_1 - \theta_{22})^2}{\theta_{22}(1 - 2\theta + 2\theta_1 + \theta_{22})}, \quad (5)$$

where all quantities are as defined in Sec. III and the coverage of hydrogen in singly occupied dimers is given by $\theta_1 = \theta - \theta_2$.

We have numerically inverted Eqs. (4) and (5) to compare with the experimental data for θ_2 and θ_{22} as a function of the total coverage θ shown in Figs. 4(a) and 4(b), as well as for the more sensitive data for the unpaired hydrogen coverage θ_1 that is displayed in Fig. 4(c). Good agreement is found for all of these quantities using appropriate values for ε and ω. The best fits are obtained for $\varepsilon/kT = 6.1$ and $\omega/kT = 0.8$. As expected from our qualitative discussion, the pairing energy is found to be significantly greater than the thermal energy, while the clustering energy is close to the thermal energy. The two dotted curves in Fig. 4(c) are calculated results changing the value of ε/kT by ± 0.6. They clearly provide a poorer fit to our experimental data. Varying the value of ω/kT also results in poorer fit, especially at low hydrogen coverages, since it strongly affects the value of θ_{22}.

2. Analysis of spatial correlation function

Except for the domain of very low H coverage, essentially all of the adsorbed hydrogen atoms are located on doubly occupied dimers. Thus, to examine the clustering interaction separately, we can consider a model in which all of the hydrogen adatoms are assumed to be paired on dimer units. Then the nearest-neighbor interaction model presented above for the dimer row reduces to a single-site lattice gas in one dimension with a nearest-neighbor interaction. This corresponds to the one-dimensional Ising model, for which a full

analytic solution is available.[36] The solution of this problem is expressed most conveniently in terms of a correlation function, rather than in terms of the equivalent cluster-size distribution. For our case the relevant correlation function is that for the hydrogen-site occupancy, i.e., the probability $p(j)$ of two dimers in one dimer row separated by j sites both being (doubly) occupied. After some adaptation, the result of the one-dimensional Ising model yields for the correlation function

$$p(j)=\theta_2^2+\theta_2(1-\theta_2)\exp\left(-j\ln\frac{\sqrt{f(\theta_2)}+1}{\sqrt{f(\theta_2)}-1}\right) \tag{6}$$

with

$$f(\theta_2)\equiv 1+4\theta_2(1-\theta_2)(e^{\omega/kT}-1). \tag{7}$$

This relation is simply that of an exponentially decaying correlation as a function of the displacement. The initial correlation for $j=0$ corresponds to θ_2 and the asymptotic value for large displacements is θ_2^2. For any given coverage, the correlation length

$$l_c\equiv 1/\ln\frac{\sqrt{f(\theta_2)}+1}{\sqrt{f(\theta_2)}-1} \tag{8}$$

increases monotonically from a value of zero to infinity as the interaction energy ω increases. For a given interaction energy, the predicted correlation length within this model approaches zero in the limit of negligible ($\theta_2\rightarrow 0$) or full ($\theta_2\rightarrow 1$) coverage. The longest correlation length will be obtained for $\theta_2=0.5$.

Figure 5 provides a comparison of this analysis with the experimentally calculated spatial correlation function $p(j)$ for the occupancy of doubly occupied dimers. The predicted exponential form for the correlation function is found to agree well with the experimental data at the two hydrogen adsorbate coverages that were examined. A relatively weak spatial correlation is observed experimentally, with appreciable correlation existing only for nearest neighbors. This behavior is reproduced for a low value of the normalized interaction energy ω/kT. The inferred clustering interaction energies from fitting the experimental data are $\omega/kT=1.0$ for an hydrogen coverage of $\theta=0.13$ ML ($\theta_2=0.12$ ML) and $\omega/kT=0.9$ for $\theta=0.26$ ML ($\theta_2=0.25$ ML).

D. Monte Carlo simulations

To provide the most stringent test of the capabilities of the nearest-neighbor interaction model to predict the experimental results, we would like to obtain information on the expected distribution not only of singly and doubly occupied dimers, but also of sizes of clusters of doubly occupied dimers. While the spatial correlation data is a complementary form of analysis that is obviously closely related to the cluster-size distribution, we were only able to analyze the correlation function analytically in the limit of infinite pairing energy (Sec. IV C 2). On the other hand, we could treat the case of both a finite pairing and clustering energy analytically (Sec. IV C 1), but only under the restriction of making a comparison with experiment at the level of the number of pairing and clustering bonds, rather than the more detailed examination of the distribution of cluster sizes. With these factors in mind, we felt it worthwhile to perform direct Monte Carlo simulations of the adsorbate configurations for the full quasi-one-dimensional model with both interactions included.

The Monte Carlo method was applied in the following manner. We first generated a random initial distribution of H adatoms at the desired coverage along a dimer row of length 1000. We then introduced hopping attempts using a random sequence generator. The elementary hopping steps are single adatom hopping events that move to an adjacent unoccupied site along the dimer row. For each tentative hopping event, the hopping probability ρ is decided according to a standard criterion[37] in which

$$\rho=\begin{cases}1, & \delta E\leqslant 0,\\ e^{-\delta E/kT}, & \delta E>0,\end{cases} \tag{9}$$

where δE is the change in energy associated with the hop.

In the simulations we typically allowed for a total of $\sim 2\times 10^9$ tentative adatom hops. While this number of hops was clearly sufficient to reach complete pairing, the clustering process might develop significantly more slowly. To ensure that we had indeed reached the equilibrium hydrogen configuration in our simulations, we carried them out under two very different assumptions for the initial-site distribution of the hydrogen adatoms. One was random; the other was a distribution resulting from a simulation using very high clustering energy $\omega=0.3$ eV, i.e., a distribution already showing strong clustering. For both initial conditions (one with too little clustering and one with too much clustering compared to the equilibrium result), we obtained equivalent results. This constitutes strong evidence that equilibrium condition was satisfied. The average number of moves to achieve equilibrium was also, we note, consistent with our experimental procedures for annealing the H-covered Si(100) sample.

A comparison of the results of the Monte Carlo simulation with the experimental data for the cluster-size distribution for a range of different total hydrogen coverages θ is shown in Fig. 3. Remarkably good agreement is obtained for all of the data for an appropriate (fixed) set of values of the interaction energies of $\varepsilon/kT=6.1$ and $\omega/kT=0.8$. Although not shown in Fig. 3, these values also allow us to reproduce the experimental results for the coverage of singly occupied dimers θ_1 that are quoted in the caption of Fig. 3. Fitting to the coverage of singly occupied dimers was very sensitive to the choice of the value of ε/kT. We infer an uncertainly in the value of ε/kT induced by statistical errors in the data of ± 0.6, as in the analytic treatment in Sec. IV C 1. If we keep ε/kT fixed at a value of 6.1, we may examine the effect of varying the clustering energy on the cluster-size distribution. A detailed comparison of this behavior for an overall hydrogen coverage of $\theta=0.49$ ML is shown in Fig. 6. As we can see, the best fit to the experimental data is obtained for $\omega/kT=0.8$. Adequate agreement is found for ω/kT as small as 0.6 or as large as 1.0. The results shown for this particular coverage are representative of the quality and sensitivity of

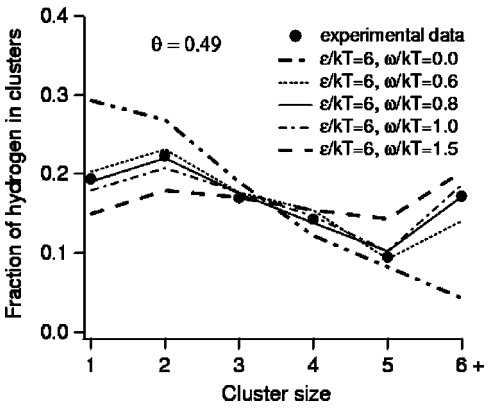

FIG. 6. Comparison of Monte Carlo simulation results for the cluster-size distribution with experimental data (points) at a hydrogen coverage of $\theta = 0.49$ ML. Calculated results are shown for $\varepsilon/kT = 6.1$ and $\omega/kT = 0.0, 0.6, 0.8, 1.0, 1.5$. The best fit is obtained for $\omega/kT = 0.8$, but reasonable agreement with the experimental data is also seen for $\omega/kT = 0.6$ and $\omega/kT = 1.0$.

the fit of the cluster-size distribution for other values of the hydrogen coverage θ. We deduce that the model adequately reproduces the experimental data for $\omega/kT = 0.8 \pm 0.2$.

E. Synopsis and preferred values of effective pairing and clustering energies

We have analyzed our experimental data within the framework of the quasi-one-dimensional nearest-neighbor model. Two analytic treatments were considered. The first allowed for finite values for both of the pairing and clustering energies, but could not predict the details of the cluster-size distribution. The second permitted analysis of the clustering effect (through calculation of the spatial correlation function), but required the approximation that full pairing was achieved. In addition, we made a direct comparison of the full model with experimental data using Monte Carlo simulations. Good agreement was obtained with the relevant experimental data for all three modes of analysis. Particularly noteworthy was the possibility, through the Monte Carlo treatment, of accurately reproducing the distribution of cluster sizes and coverage of singly occupied dimers that were obtained experimentally over a wide range of total hydrogen coverages. This could be accomplished using a single set of values for the normalized interaction energies of $\varepsilon/kT = 6.1 \pm 0.6$ and $\omega/kT = 0.8 \pm 0.2$, where the error bars follow from the quality of the fits and the uncertainty of the underlying STM counting data.

In order to relate the normalized interaction energies to the physical quantities, we must introduce the effective surface temperature for the measurement. As argued above in Sec. II, the finite quenching rate from the annealing temperature introduces some uncertainty into this quantity. The correction from the annealing temperature is expected to be modest with respect to the clustering interaction, and we simply use the annealing temperature of $T = 650$ K. It follows that $\omega = 0.04 \pm 0.01$ eV. For the pairing interaction, a reduction in the effective surface temperature to $T = 600$ K is estimated from the diffusion of unpaired hydrogen atoms. We then obtain $\varepsilon = 0.31 \pm 0.04$ eV, where an additional uncertainty of 5% has been included in the estimate from possible error in the determination of the effective surface temperature.

V. DISCUSSION AND CONCLUSIONS

At the qualitative level, our study of the equilibrium configuration of hydrogen atoms adsorbed on the Si(100) surface confirmed the presence of a strong effective interaction leading to pairing of the adatoms on Si dimers. Except at very low adsorbate coverages, most of the adsorbed H atoms were in the paired state. An attractive effective interaction between adjacent doubly occupied dimers, the so-called clustering interaction, was also discerned. It was found to be relatively weak and to give rise only to a slight clustering effect of the doubly occupied dimers. These results can be readily understood at the intuitive level by considering the separation of the two Si atoms in a single dimer of 0.23 nm compared with the larger separation of 0.38 nm between adjacent dimers along a row. Thus, the strength of corresponding π bonds, which drive the effective attractive interactions between the adsorbed species, is expected to be appreciably larger for the intradimer configuration than for the interdimer case. On a quantitative level, the effective clustering energy found in this work is considerably lower than estimated by Yang *et al.*[21] and Flowers *et al.*[22] from the previously published STM data of Boland.[10] The treatment in these works is similar to that of the present investigation; the discrepancy arises from the higher incidence of clustering apparent in the older STM images. The latter, however, do not provide the large statistical sample that was employed in the present work, nor do they readily permit assessment of—or correction for—possible effects of contamination or surface defects. In modeling of careful recent measurement of the kinetics of recombinative desorption of hydrogen, Zimmermann and Pan[23] inferred a value of $\omega = 0.06$ eV. This figure differs somewhat from our preferred value of $\omega = 0.04$ eV. The broad conclusion that this energy is not large compared with thermal energies is, however, also reached on the basis of this very different type of experimental data.

One of the interesting and, arguably, surprising aspects of the present investigation was the degree to which the nearest-neighbor interaction model was capable of reproducing the detailed experimental data on the cluster-size distribution, as well as the fraction of singly occupied dimers. Clearly such a model is highly simplified. Indeed, other kinds of interactions, such as next-nearest-neighbor interdimer interactions, have been suggested, for example, by density functional calculations.[24] How then do we understand the good agreement that we have found with the predictions of a nearest-neighbor interaction model? The answer probably lies in the fact, that to a first approximation, the behavior of the hydrogen adatoms can be described as fully paired, but with weak interdimer interactions. The basic characteristics of the system are captured by this description; the corrections are apparently adequately represented within a model of nearest-neighbor interactions. It is likely that the experimental data obtained in our measurements would also be reproduced by

more complex models of the interaction, albeit with somewhat different values for the effective nearest-neighbor interactions.

It is appropriate to make some remarks concerning the implications of our measurements on the expected kinetics for the recombinative desorption of hydrogen from Si(100) surfaces. The relatively small clustering energy suggests that a simple interdimer desorption pathway in which two hydrogen atoms from adjacent dimers react cannot explain the near-first-order kinetics seen experimentally. Nevertheless, this observation does *not* imply that ''clustering'' itself is necessarily unimportant for the desorption process. At moderate coverages a significant fraction of the adsorbed hydrogen [cf. Fig. 4(b)] is clustered despite the relatively weak interaction. The presence of adjacent doubly occupied dimers can therefore still play an important role in the desorption process, as in the recent model of 4H desorption pathway[23,29] which proceeds through an interdimer process.[26–29] Since the clustering energy, as determined in this work, is close to the thermal energy, the 4H pathway alone will lead to a desorption kinetics close to second-order, as shown by Zimmermann and Pan.[23] In the presence of a competing second reaction pathway, however, near-first-order behavior can be achieved. A complete description of the desorption process must naturally incorporate information about the relevant barriers, as well as information on the initial configuration of the adsorbed hydrogen provided by this investigation.

ACKNOWLEDGMENTS

The authors would like to thank Dr. J. Shan for important assistance with correlation function analysis and Drs. Michael Dürr and U. Höfer for valuable discussions about hydrogen desorption kinetics. We gratefully acknowledge the National Science Foundation and the ACS Petroleum Research Fund for support of this work.

*Current address: Institut für Allgemeine Physik, Vienna University of Technology, A-1040 Vienna, Austria.
†Current address: Department of Chemistry and Physics, Rowan University, Glassboro, New Jersey 08028.

[1] S.M. Gates and S.K. Kulkarni, Appl. Phys. Lett. **60**, 53 (1992).
[2] M. Niwano, J. Kageyama, K. Kinashi, I. Takahashi, and N. Miyamoto, J. Appl. Phys. **76**, 2157 (1994).
[3] W. Brenig and M. Hilf, J. Phys.: Condens. Matter **13**, R61 (2001).
[4] U. Höfer, Appl. Phys. A: Mater. Sci. Process. **63**, 533 (1996).
[5] K. Sinniah, M.G. Sherman, L.B. Lewis, W.H. Weinberg, J.T. Yates, Jr., and K.C. Janda, Phys. Rev. Lett. **62**, 567 (1989); K. Sinniah, M.G. Sherman, L.B. Lewis, and W.H. Weinberg, J. Chem. Phys. **92**, 5700 (1990).
[6] U. Höfer, L. Li, and T.F. Heinz, Phys. Rev. B **45**, 9485 (1992).
[7] M.L. Wise, B.G. Koehler, P. Gupta, P.A. Coon, and S.M. George, Surf. Sci. **258**, 166 (1991).
[8] J.A. Appelbaum, G.A. Baraff, and D.R. Hamann, Phys. Rev. B **14**, 588 (1976).
[9] M.T. Yin and M.L. Cohen, Phys. Rev. B **24**, 2303 (1981).
[10] J.J. Boland, J. Vac. Sci. Technol. A **10**, 2458 (1991); J.J. Boland, Phys. Rev. Lett. **67**, 1539 (1991).
[11] M.P. D'Evelyn, Y.L. Yang, and L.F. Suctu, J. Chem. Phys. **96**, 852 (1992).
[12] C.J. Wu and E.A. Carter, Chem. Phys. Lett. **185**, 172 (1991).
[13] P. Nachtigall, K.D. Jordan, and K.C. Janda, J. Chem. Phys. **95**, 8652 (1991).
[14] J.E. Northrup, Phys. Rev. B **51**, 2218 (1995).
[15] G.V. Hansson and R.I.G. Uhrberg, Surf. Sci. Rep. **9**, 197 (1988).
[16] L.S.O. Johansson and B. Reihl, Surf. Sci. **269/270**, 810 (1992).
[17] Y. Enta, S. Suzuki, and S. Kono, Phys. Rev. Lett. **65**, 2704 (1990).
[18] Z. Zhu, N. Shima, and M. Tsukada, Phys. Rev. B **40**, 11 868 (1989).
[19] N. Roberts and R.J. Needs, Surf. Sci. **236**, 112 (1990).
[20] J. Dabroski and M. Scheffler, Appl. Surf. Sci. **56-58**, 15 (1992).
[21] Y.L. Yang and M.P. D'Evelyn, J. Vac. Sci. Technol. A **11**, 2200 (1993).
[22] M.C. Flowers, N.B.H. Jonathan, A. Morris, and S. Wright, J. Chem. Phys. **108**, 3342 (1998).
[23] F.M. Zimmermann and X. Pan, Phys. Rev. Lett. **85**, 618 (2000).
[24] H.C. Kang, Surf. Sci. **445**, 167 (2000).
[25] A. Vittadini, A. Selloni, and M. Casarin, Phys. Rev. B **49**, 11 191 (1994).
[26] A. Biedermann, E. Knoesel, Z. Hu, and T.F. Heinz, Phys. Rev. Lett. **83**, 1810 (1999).
[27] M. Dürr, Z. Hu, A. Biedermann, U. Höfer, and T.F. Heinz, Phys. Rev. Lett. **88**, 046104 (2002).
[28] M. Dürr, A. Biedermann, Z. Hu, U. Höfer, and T.F. Heinz, Science **296**, 1838 (2002).
[29] M. Dürr, M.B. Raschke, E. Pehlke, and U. Höfer, Phys. Rev. Lett. **86**, 123 (2001).
[30] J.H.G. Owen, D.R. Bowler, C.M. Goringe, K. Miki, and G.A.D. Briggs, Phys. Rev. B **54**, 14 153 (1996).
[31] D.R. Bowler, J.H.G. Owen, K. Miki, and G.A.D. Briggs, Phys. Rev. B **57**, 8790 (1998).
[32] Y.J. Chabal, Surf. Sci. **168**, 594 (1986); Y.J. Chabal, G.S. Higashi, K. Raghavachari, and V.A. Burrows, J. Vac. Sci. Technol. A **7**, 2104 (1989).
[33] N. Kamakura, M. Shinohara, H. Watanabe, T. Kuwano, A. Seyama, Y. Kimura, and M. Niwano, Surf. Ref. Lett. **9**, 803 (2002).
[34] L.M. Struck, J. Eng Jr., B.E. Bent, G.W. Flynn, Y.J. Chabal, S.B. Christman, E.E. Chaban, K. Raghavachari, G.P. Williams, K. Radermacher, and S. Mantl, Surf. Sci. **380**, 444 (1997).
[35] M. Niwano, J. Kageyama, K. Kurita, K. Kinashi, I. Takahashi, and N. Miyamoto, J. Appl. Phys. **76**, 2157 (1994).
[36] R. J. Baxter FRS, *Exactly Solved Models in Statistical Mechanics* (Academic Press, New York, 1982).
[37] N. Metropolis, A.W. Rosenbluth, M.N. Rosenbluth, A.H. Teller, and E. Teller, J. Chem. Phys. **21**, 1087 (1953).